

VAST

Dynamical evolution of the bubble wall

Miguel Vanvlasselaer: miguel.vanvlasselaer@ub.edu

University of Barcelona, ICCUB and ERC (Grant agreement ID: 101141909)

Based on arxiv:2606.30740 with Benoit Laurent (PI)

UNIVERSITAT DE BARCELONA

Funded by the European Union

European Research Council
Established by the European Commission

ICCUB
Institut de Ciències del Cosmos
UNIVERSITAT DE BARCELONA

Outline

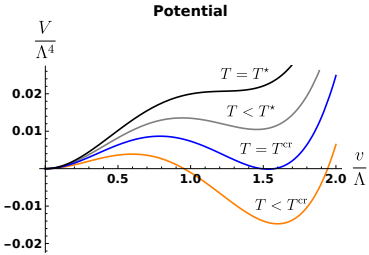
1. Pheno consequences of FOPTs
2. The pressure on the bubble wall
3. Bubble wall velocity: Static analysis
4. Bubble wall velocity: Time-dependent analysis

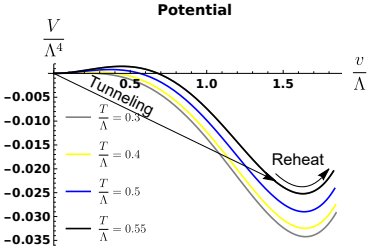
First order phase transition (FOPT) in the early universe

Universe high-T after inflation:cooling of primordial soup



- QFT = landscape of minima $\Rightarrow$ PT



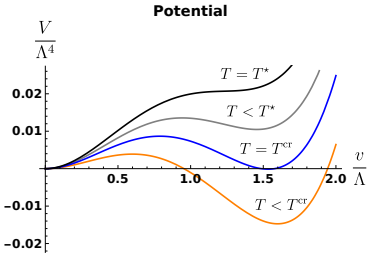


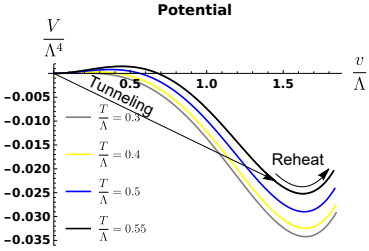
First order phase transition (FOPT) in the early universe

Universe high-T after inflation:cooling of primordial soup



- QFT = landscape of minima $\Rightarrow$ PT
- Potential $V(T,\phi) = V_0(\phi) + V_{thermal}(T,\phi)$



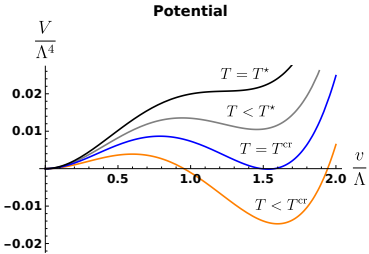


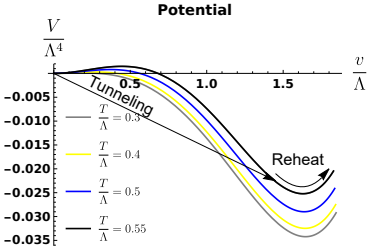
First order phase transition (FOPT) in the early universe

Universe high-T after inflation:cooling of primordial soup



- QFT = landscape of minima $\Rightarrow$ PT
- Potential $V(T,\phi) = V_0(\phi) + V_{thermal}(T,\phi)$
- High T: $V \supset \phi^2 T^2 \quad \Rightarrow$ sym restoration



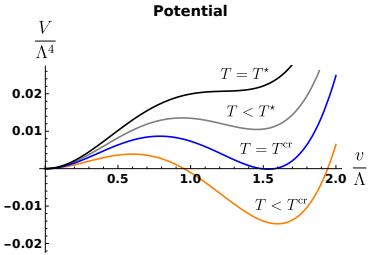


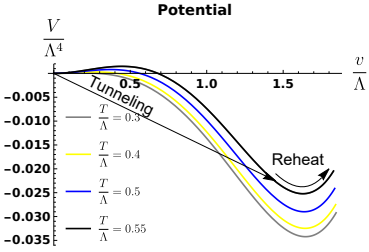
First order phase transition (FOPT) in the early universe

Universe high-T after inflation:cooling of primordial soup



- QFT = landscape of minima $\Rightarrow$ PT
- Potential $V(T,\phi) = V_0(\phi) + V_{thermal}(T,\phi)$
- High T: $V \supset \phi^2 T^2 \quad \Rightarrow$ sym restoration
- FOPT feature a barrier between two vacua and cooling ($T_{nuc} < T_{cr}$)





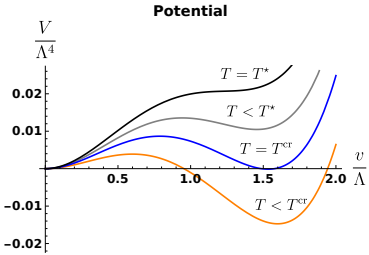
First order phase transition (FOPT) in the early universe

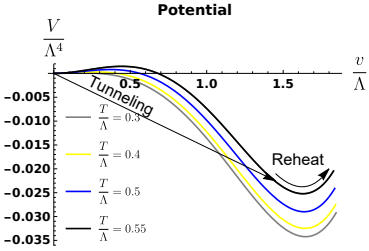
Universe high-T after inflation:cooling of primordial soup



- QFT = landscape of minima $\Rightarrow$ PT
- Potential $V(T,\phi) = V_0(\phi) + V_{thermal}(T,\phi)$
- High T: $V \supset \phi^2 T^2 \quad \Rightarrow$ sym restoration
- FOPT feature a barrier between two vacua and cooling ($T_{nuc} < T_{cr}$)
- Nucleation controlled by bounce solution

$$\Gamma \sim T^4 Exp\left[-\frac{S_3}{T}\right]$$

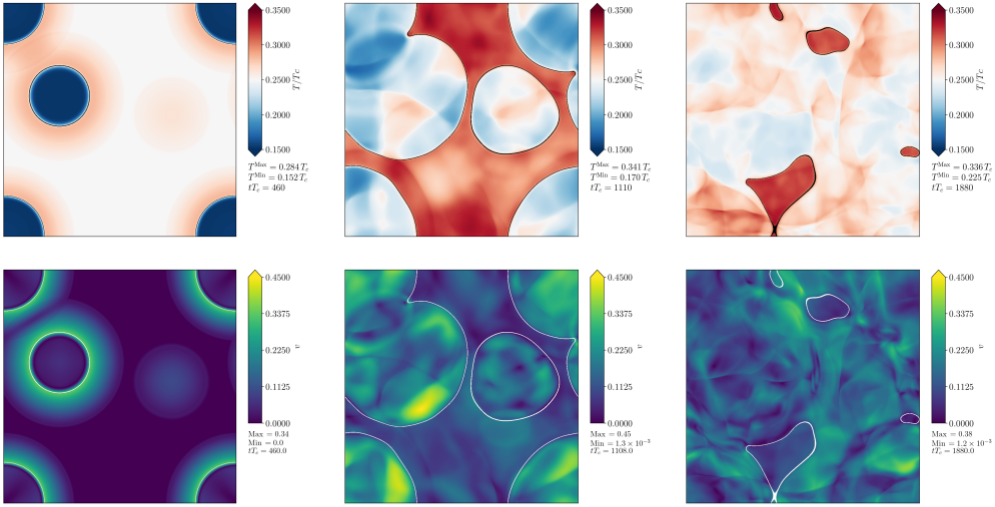




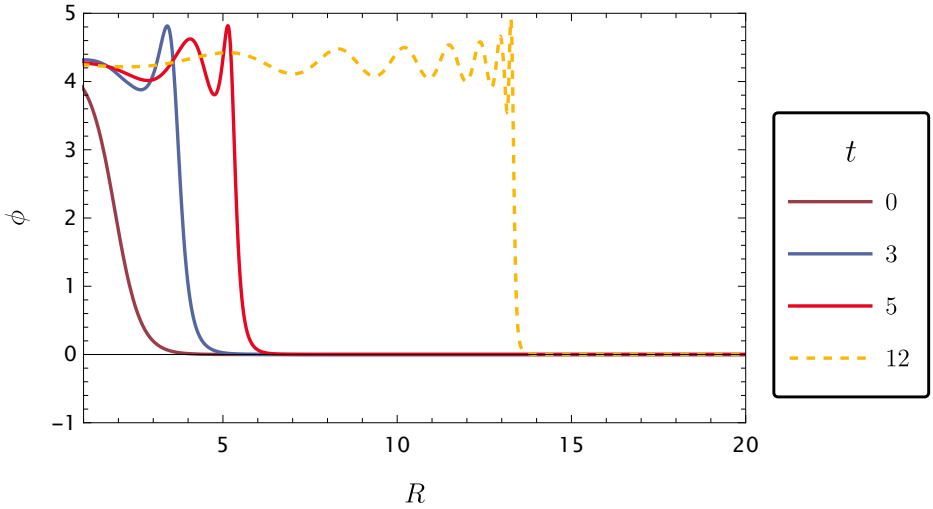
FOPT pictorially

Cutting, Hindmarsh and Weir:[1906.00480]: video in

https://vimeo.com/showcase/5968055



The bubble wall in time



Pheno consequences of FOPTs

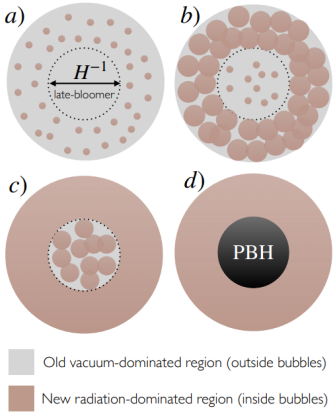
Pheno consequences of FOPTs

FOPT and PBH

1. FOPT can create a large abundance of PBH

FOPT and PBH

1. FOPT can create a large abundance of PBH
   K. Sato, M. Sasaki, H. Kodama, and K.-i. Maeda (1981-82), M. Lewicki, P. Toczek, and V. Vaskonen (2023), Gouttenoire, Volansky (2023)



FOPT and Magnetic fields

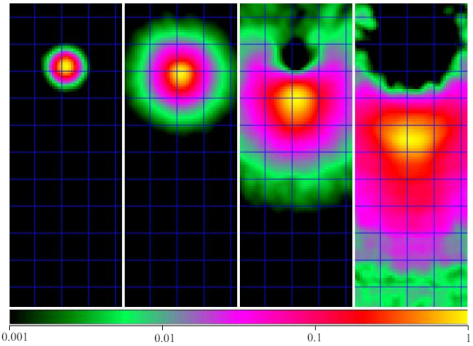
1. FOPT can create Magnetic Fields

FOPT and Magnetic fields

1. FOPT can create Magnetic Fields

   Vachaspati, Durrer, Neronov, Balaji, Fairbairn, Olea-Romacho, Vaskonen, Lewicki ...

   Suggested by Fermi-LAT/HESS (2306.05132) $B \sim 10^{-15}$ G and $\lambda \sim 1$ Mpc



In the SM from dumbbells ? 2412.00641: Brandenburg, Vachaspati

FOPT and Baryogenesis

1. Bubbles can create baryon anti-baryon asymmetry

FOPT and Baryogenesis

1. Bubbles can create baryon anti-baryon asymmetry

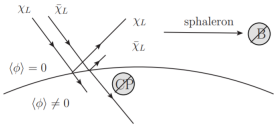
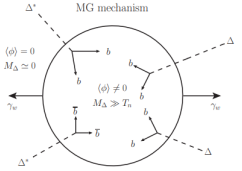
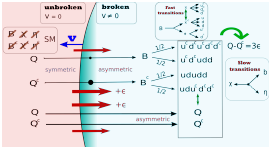


Figure: Credit:T.Konstandin [1302.6713]

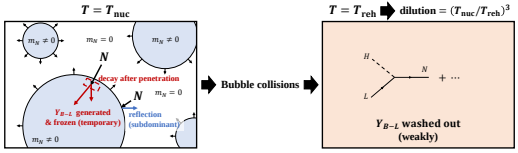


Traditional EWBG: $v_w \lesssim c_s$



Yin, Azatov, MV 21':
$\gamma_w \equiv 1/\sqrt{1-v_w^2} \gtrsim M_B^2/vT_{nuc}$

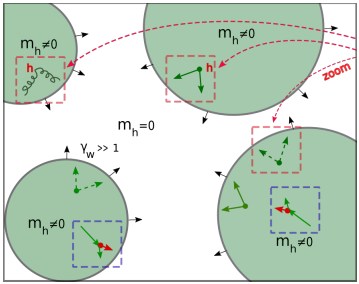
Baldes, Blasi, Mariotti, Sevrin, Turbang 21' $\gamma_w \gtrsim M_\Delta^2/vT_{nuc}$



Eung,Dutka,Jung, Nagels, MV, 23': $\gamma_w \gtrsim M_{\mathcal{RHN}}/T_{nuc}$

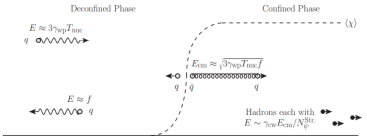
FOPT and DM

Supercool DM: Hambye, Strumia,Tesi 18'

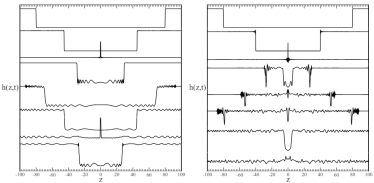


Azatov, Yin, MV 21' ,
Baldes, Sala, Gouttenoire, 22'
Azatov, Yin, Nagels, MV 24'

$$\gamma_w \equiv 1/\sqrt{1-v_w^2} \gtrsim M^2_{\mathcal{DM}}/vT_{nuc}$$



Baldes,Gouttenoire, Sala, Servant, 22' : $\gamma_w \gg 1$



Falkowski, No, 12' Giudice, Pomarol, Lee, Shakya 24' :
Runaway walls: $\gamma_w \sim M_{pf}/v \to 10^{15}$

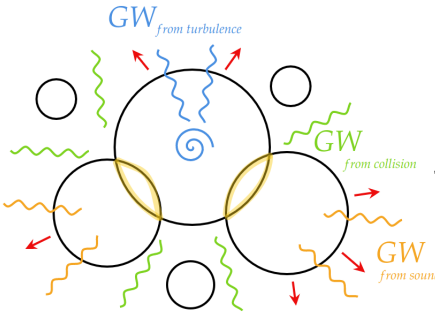
FOPT and Gravitational waves

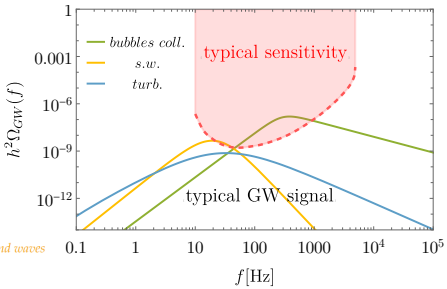
1. Bubbles can produce a stochastic GW background from

FOPT and Gravitational waves

1. Bubbles can produce a stochastic GW background from

- bubble collision
- sound waves
- turbulence





Primordial GWs could be observed soon: Frequency $\Rightarrow$ information about T_{reh}: $f_{peak} \propto T_{reh}$

Phase transition parameters for GWs

- Strength of PT: $\alpha \simeq \dfrac{\Delta V}{\rho_\gamma}$,
- Nucleation temperature T_*,
- Inverse PT duration: $\beta = (8\pi)^{1/3} R^{-1} v_w$.

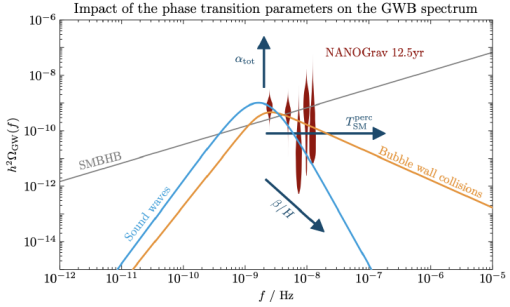


Figure: Credit: T. Bringmann et al. (2306.09411)

GW sensitivity on the PT parameters

For weak phase transitions:

$$\Omega_{gw}^{\max} \propto \left(\frac{\beta}{H}\right)^{-2} \alpha^3 v_w^5, \qquad f_{p,0} \propto \left(\frac{\beta}{H}\right) T_* v_w^{-1}$$

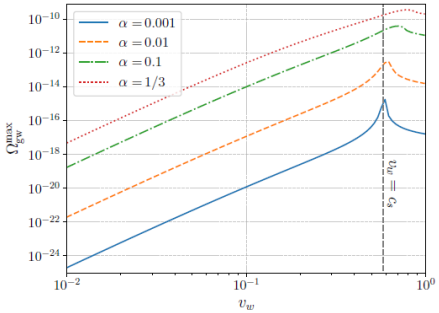


Figure: Credit: GW peak amplitude and frequency versus wall velocity

Bubble wall velocity: Static analysis

Static scalar equation of motion

The bubble dynamics is determined by the EOM

$$\partial^2\phi + \frac{\partial V_{\mathit{eff}}}{\partial\phi} + \frac{1}{2}\sum_i \frac{\partial m_i^2}{\partial\phi}\int \frac{d^3p}{(2\pi)^3 E_i}\,\delta f_i(x^\mu, p^\mu) = 0$$

Static scalar equation of motion

The bubble dynamics is determined by the EOM

$$\partial^2\phi + \frac{\partial V_{eff}}{\partial\phi} + \frac{1}{2}\sum_i \frac{\partial m_i^2}{\partial\phi}\int \frac{d^3p}{(2\pi)^3 E_i}\,\delta f_i(x^\mu, p^\mu) = 0$$

We are interested in the **late stages**, when the wall has reached a terminal velocity v_w. In the wall frame the solution is **static**:

$$\partial_t \to 0, \quad \partial^2 \to -\partial_z^2 \;\Rightarrow\; -\partial_z^2\phi + \frac{\partial V_{eff}}{\partial\phi} + \frac{1}{2}\sum_i \frac{\partial m_i^2}{\partial\phi}\int \frac{d^3p}{(2\pi)^3 E_i}\,\delta f_i = 0$$

Static scalar equation of motion

The bubble dynamics is determined by the EOM

$$\partial^2\phi + \frac{\partial V_{eff}}{\partial\phi} + \frac{1}{2}\sum_i \frac{\partial m_i^2}{\partial\phi}\int \frac{d^3p}{(2\pi)^3 E_i}\,\delta f_i(x^\mu, p^\mu) = 0$$

We are interested in the **late stages**, when the wall has reached a terminal velocity v_w. In the wall frame the solution is **static**:

$$\partial_t \to 0, \quad \partial^2 \to -\partial_z^2 \;\Rightarrow\; -\partial_z^2\phi + \frac{\partial V_{eff}}{\partial\phi} + \frac{1}{2}\sum_i \frac{\partial m_i^2}{\partial\phi}\int \frac{d^3p}{(2\pi)^3 E_i}\,\delta f_i = 0$$

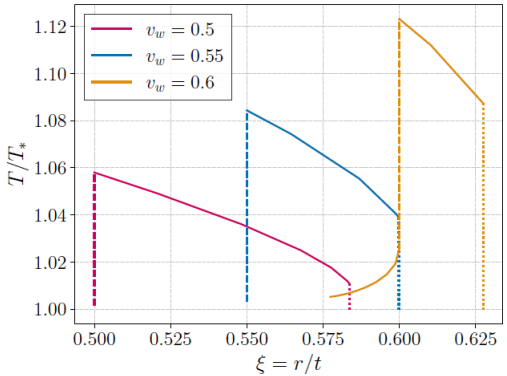
The plasma is described by energy-momentum conservation:

$$\Delta[\omega\gamma^2 v] = 0, \qquad \Delta[\omega\gamma^2 v^2 + p] = 0$$

These equations have solutions only for a **discrete set of** v_w.

Hydrodynamic obstruction

- Even in local thermal equilibrium (LTE), where $\delta f = 0$, the bubble can experience friction due to a nontrivial temperature profile $T(z)$,
- This can cause hydrodynamic obstruction preventing the wall from becoming supersonic (T. Konstandin and J. No, 1011.3735).



Hydrodynamic backreaction

- The pressure on the wall $P_{\mathcal{LTE}}$ is maximal at the Jouguet velocity v_J (fastest solution with a shock wave),
- $P_{\mathcal{LTE}}$ is discontinuous at v_J and is decreasing beyond it.

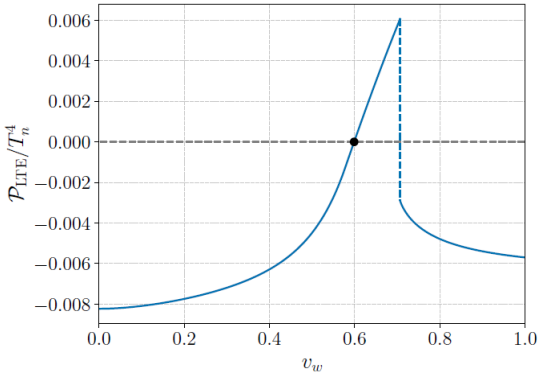


Figure: Credit: $P_{\mathcal{LTE}}/T_n^4$ versus v_w

LTE wall velocity

In LTE, entropy is conserved $\Delta[s\gamma v] = 0$, and the whole system can be described in terms of 2 parameters:

$$\alpha_p = \frac{\Delta V}{3\omega_s}, \qquad \psi = \frac{\omega_b}{\omega_s} \simeq \frac{g_*^b}{g_*^s}.$$

α_p can be interpreted as the driving force and $1 - \psi$ as the plasma-wall coupling.

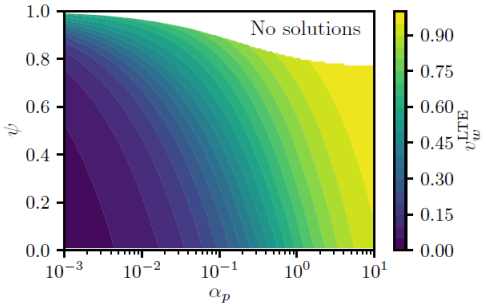
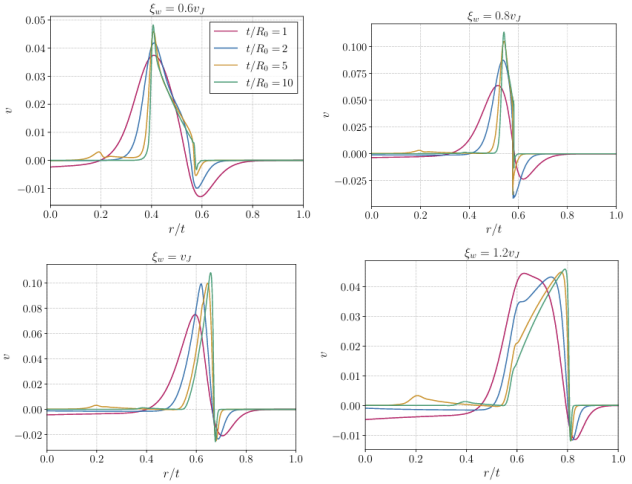


Figure: Credit: LTE wall velocity map

The formation of the shock wave

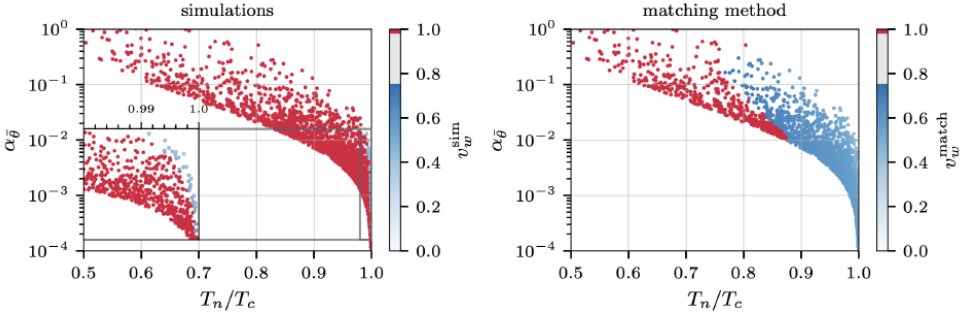
- Hydrodynamic obstruction requires a strong shock wave to form ahead of the wall.
- The static analysis assumes that this shock wave has infinite time to form.
- In a real situation, the shock wave must form before the wall reaches v_J; otherwise, hydrodynamic obstruction will not occur.
- However, $\tau_w \sim \text{few}/R_0$ and $\tau_{acc} \sim \text{few}/R_0$.



Bubble wall velocity: Time-dependent analysis

Early bubble evolution

- This was first observed in Krajewski, Lewicki and Zych (2402.15408) by doing time-dependent simulations of the early bubble evolution.
- They considered an electroweak phase transition in the singlet scalar extension, and found that hydrodynamic obstruction is much rarer than what static computations suggest.

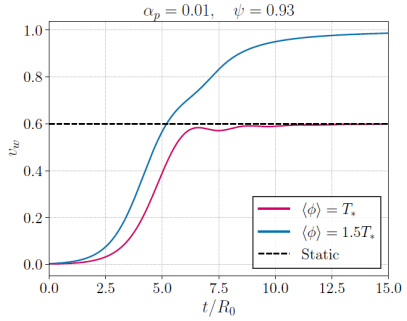


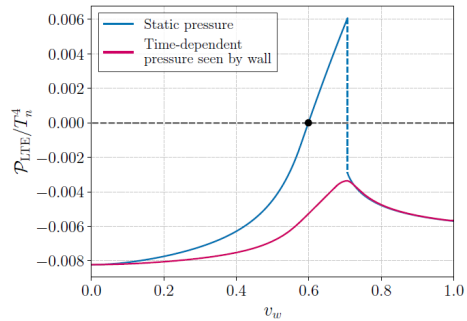
Is hydrodynamic obstruction observed in practice?

Scalar field and fluid dynamical: how does the pressure and the plasma react?

- Time-dependent simulations of bubble evolution with same α_p and ψ, but different VEV $\langle\phi\rangle$,
- Same static solution, but different early evolution.

$$\alpha_p = 0.01, \qquad \psi = 0.93$$





Maximal PT strength $\alpha_p^{\max}$

We wish to find a maximal PT strength $\alpha_p^{\max}$ such that

$$\alpha_p < \alpha_p^{\max} \Rightarrow v_w < v_J, \qquad \alpha_p > \alpha_p^{\max} \Rightarrow v_w > v_J.$$

$$\begin{aligned} \alpha_{p,max}^{SS,bag} &= \frac{1 - 2\sin^2\left(\frac{1}{3}\arcsin\psi\right)}{5 - 6\cos^2\left(\frac{1}{3}\arcsin\psi\right)} - \frac{1-\psi}{3} \\ &= \frac{10}{9\sqrt{3}}(1-\psi)^{3/2} + \mathcal{O}((1-\psi)^2). \end{aligned}$$

Model independent numerical results in the space $\alpha - \psi$

The best fit is

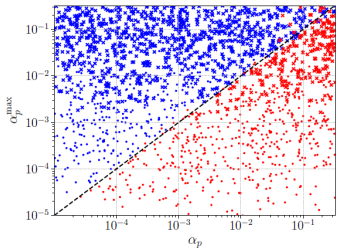
$$\alpha_{p,\max}^{dyn} \approx 8.86 \sqrt{\omega_s / T_*^4} \left(\frac{1-\psi}{\langle \phi \rangle / T_*} \right)^3$$

This is parametrically smaller (for small $1-\psi$) than the static prediction

$$\alpha_{p,\max}^{static} \approx 0.91 \, (1-\psi)^{3/2}.$$

In general, we use

$$\alpha_p^{\max} = \min \left(\alpha_{p,\max}^{static}, \, \alpha_{p,\max}^{dyn} \right)$$



- Blue: $v_w < v_J$
- Red: $v_w > v_J$

Time-dependent analysis

We use the **Nambu-Goto** EOM to get a rough time-dependent analytical description:

$$\gamma_R^3 \ddot{R} + \frac{d-1}{R}\gamma_R = \frac{\mathcal{P}(t)}{\sigma},$$

with

$$\mathcal{P}(t) = \int dr\, \partial_r \phi \, \frac{\partial V_{eff}(\phi, T)}{\partial \phi},$$
$$\sigma = \frac{1}{\gamma_R}\int dr\, (\partial_r \phi)^2 \sim \frac{\langle \phi \rangle^2}{L}.$$

To get a simple analytical estimate, it is sufficient to work in the **thin-wall limit**, where we assume a planar wall ($d = 1$).

Analytical understanding of the pressure evolution

- $\mathcal{P}(t)$ is difficult to evaluate because $\partial V_{\mathit{eff}}/\partial\phi$ depends on a nontrivial temperature profile $T(t,z)$,
- However, it can be expanded around $t=0$, where $T(0,z)=T_*$:

$$\mathcal{P}(t) = \mathcal{P}(0) + \partial_t\mathcal{P}(0)\,t + \frac{1}{2}\partial_t^2\mathcal{P}(0)\,t^2 + \mathcal{O}(t^3)$$

with

$$\begin{aligned}
\mathcal{P}(0) &= \Delta V \sim \alpha_p\,\omega_s, \\
\partial_t\mathcal{P}(0) &= 0, \qquad \text{(because } \partial_t R(0)=0\text{)} \\
\partial_t^2\mathcal{P}(0) &= -\int dz\,\partial_z\phi\,\partial_t^2 T\,\frac{\partial^2 V_{\mathit{eff}}}{\partial\phi\,\partial T}\bigg|_{t=0} \\
&= -\partial_t^2 R(0)\int dz\,(\partial_z\phi)^2\left(\frac{\partial^2 V_{\mathit{eff}}}{\partial\phi\,\partial T}\right)^2\left(\frac{\partial^2 V_{\mathit{eff}}}{\partial T^2}\right)^{-1}\bigg|_{t=0} \\
&\sim -(1-\psi)^2\,\alpha_p\,\langle\phi\rangle^{-2}\,\omega_s^2
\end{aligned}$$

Maximal α_p for hydrodynamic obstruction

$$\max_t [\gamma_w v_w] \sim \frac{\langle \phi \rangle \, \alpha_p^{1/3}}{(1-\psi)\, \omega_s^{1/6}\, T_*^{1/3}}$$

We now assume that walls with a maximal velocity below some fixed threshold will experience hydrodynamic obstruction. Inverting for α_p, we get

$$\alpha_p^{\max} = c \sqrt{\omega_s / T_*^4} \left(\frac{1-\psi}{\langle \phi \rangle / T_*} \right)^3,$$

with c some numerical factor to be determined numerically.

According to this analysis, walls with $\alpha_p < \alpha_p^{\max}$ will experience hydrodynamic obstruction and have $v_w < v_J$. Otherwise, they become relativistic.

Discussion

- Although the static analysis provides correct solutions, it cannot tell which solution is realized in practice. This can only be determined from dynamical analysis,
- At small $1-\psi$, the LTE hydrodynamic obstruction is **much weaker** than previously thought,
- This agrees with the xSM analysis of 2402.15408 which had $1-\psi \sim 0.01$,
- We did not include **dissipative effects**, which generally create more friction and slow down the wall, so the real $\alpha_p^{\max}$ should be larger,
- We also neglected nonspherical modes, although their effects are still not understood.

Thank you!

Toy model: High-T potential

$$V_{\mathcal{H}T}(\phi, T) = \frac{a}{12}\left(\phi^2\left[6v_b^2 - 4v(1+b)\phi + 3\phi^2\right] - \omega_* \frac{T^4}{T_*^4} + \frac{c}{4}(T^2 - T_*^2)\phi^2\right),$$

$$\omega_* = \frac{2\pi^2}{45} g_* T_*^4, \quad a = \frac{9\alpha_p \omega_*}{(1-2b)v^4}, \quad c = \frac{(1-\psi)\omega_*}{T_*^2 v^2}.$$

- These follow by inverting $\alpha_p \equiv 4\Delta V/(3\omega_*)$ and $\psi \equiv \omega_b(T_*)/\omega_s(T_*) \simeq g_*^b/g_*^s$.
- b controls the barrier height and is obtained by requiring S_3/T_* to equal a constant (e.g. $\simeq 140$).

Toy Model: Constant acceleration

Scalar field imposed by hand, fluid dynamical: how does the pressure and the plasma react?

We set the wall by hand with a constant acceleration A and simulate the plasma around it:

$$\mathcal{P}_{\mathcal{LTE}} = \int dr\, \partial_\phi r(\phi) \left(\frac{\partial V_0(\phi)}{\partial \phi} + \sum_i \frac{\partial \eta_i^2(\phi)}{\partial \phi} \right) \int \frac{\partial^3 p}{(2\pi)^3 2E_i} f_i(p, x, T)_{\mathcal{R}} \tag{1}$$

However, in the context of a plasma which is in local thermal equilibrium, one can again interpret

$$\mathcal{P}_{\mathcal{LTE}}(t) = \int_0^{+\infty} dr\, \partial_\phi r(r,t) \frac{\partial V_{\mathit{eff}}(\phi, T)}{\partial \phi}\bigg|_{(\phi(r,t),\, T(r,t))} . \tag{2}$$

